https://doi.org/10.5194/esd-2019-58
Preprint. Discussion started: 2 October 2019

Earth System Dynamics
Discussions
Open Access
EGU

Using a nested single-model large ensemble to assess the internal variability of the North Atlantic Oscillation and its climatic implications for Central Europe

Andrea Böhnisch[1], Ralf Ludwig[1], and Martin Leduc[2, 3]

[1]Department of Geography, Ludwig-Maximilians-Universität München, Munich, Germany
[2]Ouranos, Montréal,Québec, Canada
[3]Centre ESCER, Université du Québec à Montréal, Montréal, Québec, Canada

Correspondence: Andrea Böhnisch (a.boehnisch@iggf.geo.uni-muenchen.de)

Abstract. Central European weather and climate is closely related to atmospheric mass advection triggered by the North Atlantic Oscillation (NAO) which is a relevant index for quantifying natural variability on multi-annual time scales. It remains unclear, though, how large-scale circulation variability affects local climate characteristics when downscaled using a regional climate model. In this study, 50 members of a single-model initial-condition large ensemble (LE) (www.climex-project.org) are analyzed for a climate–NAO relationship, especially its inter-member spread and its transfer from the driving model CanESM2 into the driven model CRCM5. The NAO pressure dipole is quantified in the CanESM2-LE by an extended station-based index; responses of mean surface air temperature and total precipitation to changes in the index value are determined for a Central European domain (CEUR) in both the CanESM2-LE and CRCM5-LE. NAO–response relationships are expressed via Pearson correlation coefficients (strength) and the change per unit index change for historical (1981–2010) and future (2070–2099) winters. Results show that (a) statistically robust NAO patterns are found in the CanESM2-LE under current forcing conditions and (b) impulses from the NAO in the CanESM2-LE produce correct responses in the high-resolution CRCM5-LE. Relationships weaken in the future period, but the amplitude of their inter-member spread shows no significant change. Among others, the results strengthen the validity of the climate module in the ClimEx model chain for further impact modelling and stress the importance of single-model ensembles for evaluating internal variability.

1 Introduction

One of the major sources of uncertainty regarding short-term future climate projections is internal climate variability, while model climate response and greenhouse gases concentrations scenarios become more important sources of uncertainty on a longer-term time horizon (Hawkins and Sutton, 2009, 2011). The term internal variability denotes variability which is not forced by external processes (either anthropogenic or natural), but arises from the chaotic properties of the climate system itself (Leduc et al., 2019; Deser et al., 2012). One way to trigger internal variability in global climate model (GCM) simulations is to apply slight differences in the initial conditions of the model, leading to varying sequences of weather events with similar long-term climate statistics.

https://doi.org/10.5194/esd-2019-58
Preprint. Discussion started: 2 October 2019

Earth System Dynamics Discussions
Open Access
EGU

Global atmospheric modes of variability alter the sequences of weather events through the linking between large-scale circulation and local weather characteristics (like surface air temperature and precipitation). They can thereby establish periods of discernible states on multi-annual time scales. Among these modes, the North Atlantic Oscillation (NAO) is particularly important for northern hemisphere climate. Its two states, positive and negative, are accompanied by a stronger and weaker pressure gradient, respectively, over the North Atlantic region (Hurrell and Deser, 2009). They are evoked by planetary wave-breaking in the polar front, leading to antagonistic pressure behaviour of two centres over the North Atlantic: one located within the subtropical high pressure belt ("Azores High", AH), the second in subpolar regions ("Icelandic Low", IL) (Benedict et al., 2004). The resulting pressure gradient affects large-scale extra-tropical circulation, especially the strength and position of mid-latitude westerly winds connected to the jet stream, and air mass advection during boreal winter (Deser et al., 2016; Hurrell and Deser, 2009).

Commonly, the NAO is quantified with an index making use of this pressure gradient between AH and IL. The index may be calculated as a normalized difference of sea level pressure or geopotential height station measurements, spatially averaged pressure values of pre-set regions, or the region of highest pressure variance is obtained by principal component analysis (Pokorná and Huth, 2015; Hurrell and Deser, 2009; Stephenson et al., 2006; Hurrell, 1995; Rogers, 1984). Each method has its advantages and limitations (see e.g. Pokorná and Huth, 2015, for a detailed survey of various approaches).

The positive state leads to warmer and moister winters in Northern Europe, but cooler and drier conditions in the South, and vice versa in the negative state (e.g., Hurrell and Deser, 2009; Pokorná and Huth, 2015; Woollings et al., 2015). Several feedbacks with other teleconnection patterns, like El Niño/Southern Oscillation, and with the ocean circulation are reported (Hurrell and Deser, 2009; Moore et al., 2013). Further on, high pressure regions over Greenland (Greenland blocking) are likely related to the emergence of negative NAO phases (Hanna et al., 2015).

While the typical NAO pattern and its impacts are usually correctly reproduced in GCMs (Stephenson et al., 2006; Ulbrich and Christoph, 1999; Reintges et al., 2017), its dynamics in a future climate remain uncertain: the NAO is found as intensifying, but also counteracting global warming in the northern hemisphere ("global warming hiatus") (Iles and Hegerl, 2017; Deser et al., 2016; Delworth et al., 2016). Similarly, the findings regarding the prevalence of future positive or negative states lack unity: Analyses of CMIP5 models, for example, suggest an increase of positive phases under rising greenhouse gas concentrations until 2100 (e.g., Woollings et al., 2010; Kirtman et al., 2013; Christensen et al., 2013). On the other hand, due to reduced sea ice extents which seem to be occasionally coupled with Greenland blocking, negative NAO phases may become more likely in future climate (Gillett and Fyfe, 2013; Hanna et al., 2015).

It is common in most of the mentioned studies to rely on one simulation per model and estimate its performance by this single run. This approach allows for comparing different models (and observations). However, it is not possible to directly evaluate the range of the model internal NAO variability, or whether the chosen simulation is a good representation of how this model simulates the phenomenon in question (Leduc et al., 2019). Single realizations of a given model may vary considerably among themselves (and deviate from the climate evolution observed in reality), such that relying on single realizations possibly deteriorates the assessment of a given model.

Due to their coarse spatial resolution GCMs are poorly resolving land–water contrasts and topographic properties which may

https://doi.org/10.5194/esd-2019-58
Preprint. Discussion started: 2 October 2019


Earth System Dynamics Discussions Open Access EGU

be highly relevant in climate impact studies over heterogeneous landscapes (Leduc et al., 2019). Thus, dynamical downscaling is advised, using a regional climate model (RCM) (Leduc et al., 2019). It is however not clear, how global circulation variability affects local climate characteristics when downscaled using an RCM and whether the range of internal variability (i. e., the inter-member spread of the LE) is transferred correctly from the driving GCM into the driven RCM. This question may be important for impact modellers who work with RCM data without taking the driving GCM into account.

This study is analysing the NAO in a very large single-model ensemble: the 50 GCM members driving an RCM within the Climate Change and Hydrological Extremes (ClimEx) project (Leduc et al., 2019). It allows for analysing the spread of NAO states and responses within one model chain, thus establishing the range of internal variability of the NAO, and finding robust NAO patterns which exceed the uncertainty due to internal variability in the ensemble. So this study is focussing on four topics and related key questions:

(a) General performance of the model chain: Can the driving GCM resolve the NAO correctly and are climatic implications for Central Europe reproduced?

(b) Internal Variability: What is the range of possible NAO patterns, displayed by the variances among the 50 members?

(c) Nesting approach: Do GCM NAO impulses propagate correctly into the RCM realizations and produce realistic response patterns?

(d) Climate change: How do (a), (b) and (c) change in transient climate simulations until 2099 using an RCP8.5 emissions scenario?

This paper is structured as follows: Sect. 2 introduces data and methods and Sects. 3 and 4 present and discuss the results, respectively, followed by conclusions in Sect. 5.

2 Data and Methodology

2.1 Data

Data from three different sources are employed in this study (Table 1). The major source is the ClimEx data set which is described in detail in Leduc et al. (2019). The ClimEx project (www.climex-project.org) is conducted in a Québec-Bavarian cooperation and targets issues of hydrological extreme events in the time horizon of 1950–2099, using a high-resolution 50 member single-model initial-condition large ensemble with an RCP8.5 emissions scenario from 2006 onwards (Leduc et al., 2019). This single-RCM 50-member ensemble allows for internal variability and extreme events to be detected in high spatial and temporal resolution within a total of 7500 modelled years (Leduc et al., 2019). The members are assumed to become independent about five years after their initialization in 1950 (spin-up-period) (Leduc et al., 2019).

As described in Leduc et al. (2019), the original 50 members of the Canadian Earth System Model version 2 (CanESM2

https://doi.org/10.5194/esd-2019-58
Preprint. Discussion started: 2 October 2019

Earth System Dynamics
Discussions
Open Access
EGU

Table 1. Overview of used data sets, their spatial resolution, the number of members and the employed variables.

data name	model type	spatial resolution	members	variables
ERA-I	re-analysis	$0.75^\circ \times 0.75^\circ$	1	msl [Pa], t2m [K], tp [m]
CRCM5/ERA-I	RCM	$0.11^\circ \times 0.11^\circ$	1	tas [K], pr [$\mathrm{kgm^{-2}s^{-1}}$]
CanESM2	GCM	$2.8^\circ \times 2.8^\circ$	50	psl [Pa], tas [K], pr [$\mathrm{kgm^{-2}s^{-1}}$]
CRCM5-LE	RCM	$0.11^\circ \times 0.11^\circ$	50	tas [$^\circ$C], pr [mm]

Large Ensemble, 2.8° spatial resolution, Fyfe et al., 2017) have been downscaled using the Canadian Regional Climate Model version 5 (CRCM5 Large Ensemble, 0.11° spatial resolution) over two domains in Europe and north-eastern North America. During the nesting process large-scale spectral nudging regarding the horizontal wind field was applied (Leduc et al., 2019). Comparing the single-model internal variability of the CRCM5 members with the inter-model spread of the CORDEX ensemble regarding winter temperature and precipitation, von Trentini et al. (2019) have shown that both ensemble spreads are of comparable magnitude. This similarity suggests that a large fraction of the CORDEX ensemble spread can be explained by internal variability, despite the fact that it was not explicitly sampled within the CORDEX framework (where most models provided a single simulation). Therefore, the ClimEx ensemble can be expected to capture the most important expressions of natural variability.

The ERA-Interim Reanalysis data set of the European Centre for Medium-Range Weather Forecasts (ECMWF) serves as a reference (REF; Dee et al., 2011) and the CRCM5/ERA-I run was used to evaluate the CRCM5 under "perfect" (as far as ERA-I can be assumed as representing reality) lateral boundary conditions, i.e. without the potential CanESM2 input data error.

The relevant variables for this study are:

- (mean) sea level air pressure (msl, psl, referred to as "psl", in [hPa]) to obtain the NAO,
- near surface air temperature (t2m, tas, referred to as "tas", in [K]),
- total precipitation including liquid and solid precipitation from all types of clouds (tp, pr, referred to as "pr", in [mm]).

Commonly, NAO impact studies focus on seasonally aggregated values of the analyzed variables or extreme events (e.g., Stephenson et al., 2006). Yet the NAO which accounts for variations in the mean zonal atmospheric flow towards Europe can be assumed not only to influence winter mean values, but also their scattering. So the following analyses are not limited to winter mean temperature (tas mean) and precipitation sums (pr sum), selected analyses were also performed on winter mean monthly standard deviations of daily mean temperature (tas std) as a measure of temperature variation.

https://doi.org/10.5194/esd-2019-58
Preprint. Discussion started: 2 October 2019


Earth System Dynamics Discussions
Open Access
EGU

2.2 Methodology

This section gives an overview of the selection of regions and time horizons, the derivation of the employed NAO index as well as corresponding, spatially varying climatic responses in Central Europe and the quantification of internal variability within the study.

2.2.1 Regions of interest and time horizon selection

Analyses were performed on time series of spatially averaged information (tas mean, pr sum for response variables and psl for index calculation) and spatially explicit data (tas mean, tas std, pr sum). All data were provided as netCDF and most pre-processing was performed using the Climate Data Operators (CDO) of the Max-Planck-Institute for Meteorology (Schulzweida, 2017).

Within this study, there are two separated regions of interest. The first captures the formation region of the NAO over the North Atlantic using the ERA-I and CanESM2-LE dataset, while the second one is understood as the response region over Central Europe in ERA-I, CRCM5/ERA-I, CRCM5-LE and CanESM2-LE. Their properties – extent and size in terms of model-specific grid cells – are summarized in Table 2.

AH and IL regions are centred over Ponta Delgada/Azores and Reykjavik/Iceland, two commonly used stations for NAO index calculations. To avoid micro-climatic impacts and to account for moving psl centres, both NAO core regions were extended to a 3×3 GCM grid cell matrix each. The NAO index proved to be very robust towards the exact shape of the core regions.

Similar to the pressure centres, the Central European domain (CEUR) was defined for CanESM2-LE by selecting a 5×5 GCM grid cell matrix centred over Munich/Germany. This CEUR domain extends from Denmark in the north to mid-Italy in the south and from Poland to France in east–west direction. The corresponding CEUR region in the ClimEx European domain (Leduc et al., 2019) was used to quantify the impacts of the NAO in the CRCM5-LE dataset. It lies downstream of the westerly flows initiated by the NAO, so the following analyses will set a special focus on the incorporation of large-scale inflow from the western side into the nested RCM.

As the responses to NAO impulses are expected to vary over the CEUR domain, it is favourable to analyze spatial structures explicitly in addition to analyses of time series over several subset regions. These subset regions (see e.g. Déqué et al., 2007) denote small-scale areas, sized one GCM grid cell each, with expected typical “northern European” (NE) and “southern European” (SE) NAO responses for a more detailed statistical analysis. A third GCM grid cell was chosen to represent the transition zone between NE and SE. Coincidentally, it closely represents the region of Bavaria which is why the name “BY” was assigned to it. The position and size of these subset regions may be derived from Table 2 and Fig. 2. REF and RCM data is spatially averaged over several grid cells.

This study focused on inter-annual analyses which were conducted for two time horizons covering 30 years each. The chosen period length was assumed to include major fluctuations, like several solar cycles or internal climate variations. Thus a representative distribution of NAO events can be expected. Relationships between the NAO and weather variables most prob-

https://doi.org/10.5194/esd-2019-58
Preprint. Discussion started: 2 October 2019

Earth System Dynamics Discussions
Open Access
EGU

Table 2. Regions of interest: properties. Left block: limiting coordinates, right block: count of grid cells within each region. Size of grid cells: see Table 1. Abbreviations are as follows: AH – Azores High; IL – Icelandic Low; NAR – large-scale North Atlantic region for psl composites; CEUR – central Europe; NE – northern Europe; BY – Bavaria; SE – southern Europe; N/S – northern/southern border; E/W – eastern/western border.

region	N	E	S	W	ERA-I	CanESM2	CRCM5
AH	42.0°N	21.0°E	33.5°N	29.6°W	12×12	3×3	–
IL	67.1°N	18.1°E	58.6°N	26.8°W	11×11	3×3	–
NAR	75.3°N	18.3°E	30.7°N	60.5°W	105×60	28×16	–
CEUR	55.8°N	18.3°E	41.7°N	4.1°W	19×19	5×5	129×128
NE	55.8°N	12.7°E	53.0°N	9.8°W	3×4	1	25×26
BY	50.3°N	12.7°E	47.4°N	9.8°W	3×4	1	26×26
SE	44.7°N	12.7°E	41.7°N	9.8°W	3×4	1	26×26

ably vary on different time scales (Hurrell and Deser, 2009; Woollings et al., 2015; Xu et al., 2016; Hurrell and Van Loon, 1997). However, as 30 year periods are not long enough for analyses of multidecadal (>30 years) NAO–response variability (Woollings et al., 2015), stationarity in NAO patterns and impacts was assumed for simplicity reasons.

The historical (hist; 1981–2010) period was used to establish reference statistics with ERA-I data and the ERA-I driven CRCM5 run. These statistics were evaluated in GCM and RCM data to check the models' ability of depicting NAO responses. Links and relationships established for the historical period were also investigated in a far future horizon (2070–2099).

All data (spatially explicit and subset time series) was aggregated to the seasonal time scale (winter means for tas and winter sums for pr). Since the NAO is known to be strongest in winter (Hurrell and Deser, 2009) and the connection between station-based indices and NAO responses tends to be best in winter (see Pokorná and Huth, 2015, for months DJF), analyses were performed for months December, January, February and March (DJFM). First tests had shown that correlations and links between the NAO index and the climate variables were more distinct from noise, if March was included as well. That is why an extended winter season was used here (see also Iles and Hegerl, 2017; Hurrell, 1995).

2.2.2 Deriving an NAO index

The NAO index was derived from ERA-I and CanESM2-LE data, resulting in 1 REF and 50 model realizations. The index constructed in this study is closest to a station-based or zonally averaged index. This allowed obtaining an index in a large data set (historical and future) at justifiable computational time. It is also easy to interpret in terms of atmospheric physics. The time series of AH and IL originated from the temporally shortened and spatially averaged psl time series of both grid cell matrices for REF and GCM data only. As the CRCM5 domain does not cover the NAR-region (Leduc et al., 2019), the index can not be derived from this data source.

https://doi.org/10.5194/esd-2019-58
Preprint. Discussion started: 2 October 2019

Earth System Dynamics Discussions

Daily psl values were averaged to monthly means (Cropper et al., 2015) and scaled to obtain average $\mu = 0$ and standard deviation $\sigma = 1$, as outlined in Osborn (2004) and Hurrell and Van Loon (1997), by subtracting the 1981–2010 seasonal mean (overbar) and dividing by the 1981–2010 seasonal standard deviation (s_{IL}, s_{AH}):

$$\mathrm{NAO-Index} = \frac{AH - \overline{AH}}{s_{AH}} - \frac{IL - \overline{IL}}{s_{IL}} \tag{1}$$

Monthly indices were next averaged to DJFM means. This approach is similar to Woollings et al. (2015) and Jones et al. (2003). To compare future with historical index values, the future time series of AH and IL were normalized with the present psl standard deviations (see also Ulbrich and Christoph, 1999; Hansen et al., 2017) and mean values. The normalization of each GCM member is carried out individually, such that each member has specific normalization parameters.

2.2.3 Assessing Climatic Changes Associated with NAO

All data sources (Table 1) were used to obtain response patterns of the given variables. Climatic changes associated with NAO impulses were evaluated using Pearson correlation coefficients and a slope parameter obtained by linear regression. ERA-I and CRCM5/ERA-I tas and pr spatial data and subset region time series were correlated with the ERA-I index time series, CanESM2 and CRCM5 members were correlated with the CanESM2 index calculated for the corresponding member. The correlation analysis assumes (symmetric) linear relationships between the NAO index and tas or pr. So the associated response of the variables to NAO changes can be expressed by the linear equation (Iles and Hegerl, 2017; Stephenson et al., 2006; Hurrell, 1995):

$$Y = \alpha_1 X + \alpha_0 + \varepsilon_Y \tag{2}$$

with Y being the (response) variable at a given grid cell that is partly explained by the NAO (X, the predictor) and by any other influences (ε_Y; Stephenson et al., 2006; von Storch and Zwiers, 2003). The coefficient α_1 was estimated on each grid cell using ordinary least squares regression with the R function lm. It represents the average change in tas or pr that accompanies one unit index change during the time period under consideration (Iles and Hegerl, 2017). The line offset α_0 in Eq. (2) equals the long-term mean. The α_1 coefficients may be computed with respect to normalized index series (von Storch and Zwiers, 2003), but in this study the non-normalized index time series was preferred in order to take into account the member-specific index units.

2.2.4 Addressing Internal Variability

The NAO–response relationship was analyzed individually for each GCM and RCM member (as is done e.g. in Woollings et al., 2015). Ensemble averages partly mask internal model noise (Zwiers and von Storch, 2004), but also the spread of internal variability which this study is addressing. Nevertheless, for illustrating purposes the results were aggregated to ensemble averages (like in Deser et al., 2016). In order to avoid suppressing ensemble scattering in the spatial approach, the inter-member

https://doi.org/10.5194/esd-2019-58
Preprint. Discussion started: 2 October 2019

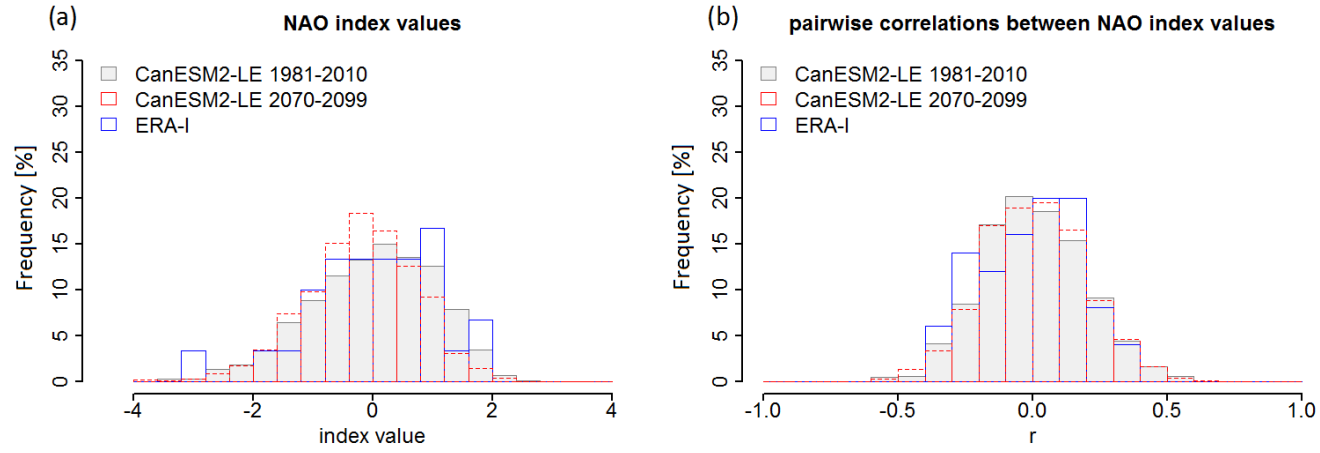

Figure 1. Comparison of CanESM2-LE and ERA-I NAO index values. Left: distribution of all CanESM2-LE (grey for 1981–2010 and red for 2070–2099) and ERA-I (blue) NAO index values. Right: distribution of pairwise correlations between all 50 CanESM2-LE member NAO index time series (grey for 1981–2010 and red for 2070–2099) and CanESM2-LE members with ERA-I (blue).

spread is represented in terms of the standard deviation of all 50 members on a given grid cell (std.dev50, see also Leduc et al., 2019; Déqué et al., 2007).

3 Results

3.1 NAO within the ClimEx Data Set

3.1.1 NAO index and psl conditions

First, a REF index was calculated from the ERA-I reanalysis. It is found to be in good accordance with often cited NAO indices like the time series of Hurrell ($r = 0.95$; index available at https://climatedataguide.ucar.edu/climate-data/hurrellnorth-atlantic-oscillation-nao-index-station-based) and therefore serves as a reference.

The CanESM2-LE produces NAO index values which follow a distribution similar to the ERA-I data (centred over zero, slight left-skewness), though the CanESM2-LE distribution appears smoother due to a larger sample size (see Fig. 1 (a)). Maximum and minimum values of some of the 50 members exceed those of the REF realization; thus, the REF realization comfortably lies within the ensemble spread. The future NAO index shows a similar distribution of values, but with slightly less positive and more negative values.

Pairwise correlations between the members and between each member and the ERA-I time series in general are not strong as can be seen in Fig. 1 (b), highlighting the independence of the CanESM2-LE members in terms of internal variability (see also Fig. A6). It is also visible that correlations among members are not stronger or weaker than correlations of members and

https://doi.org/10.5194/esd-2019-58
Preprint. Discussion started: 2 October 2019

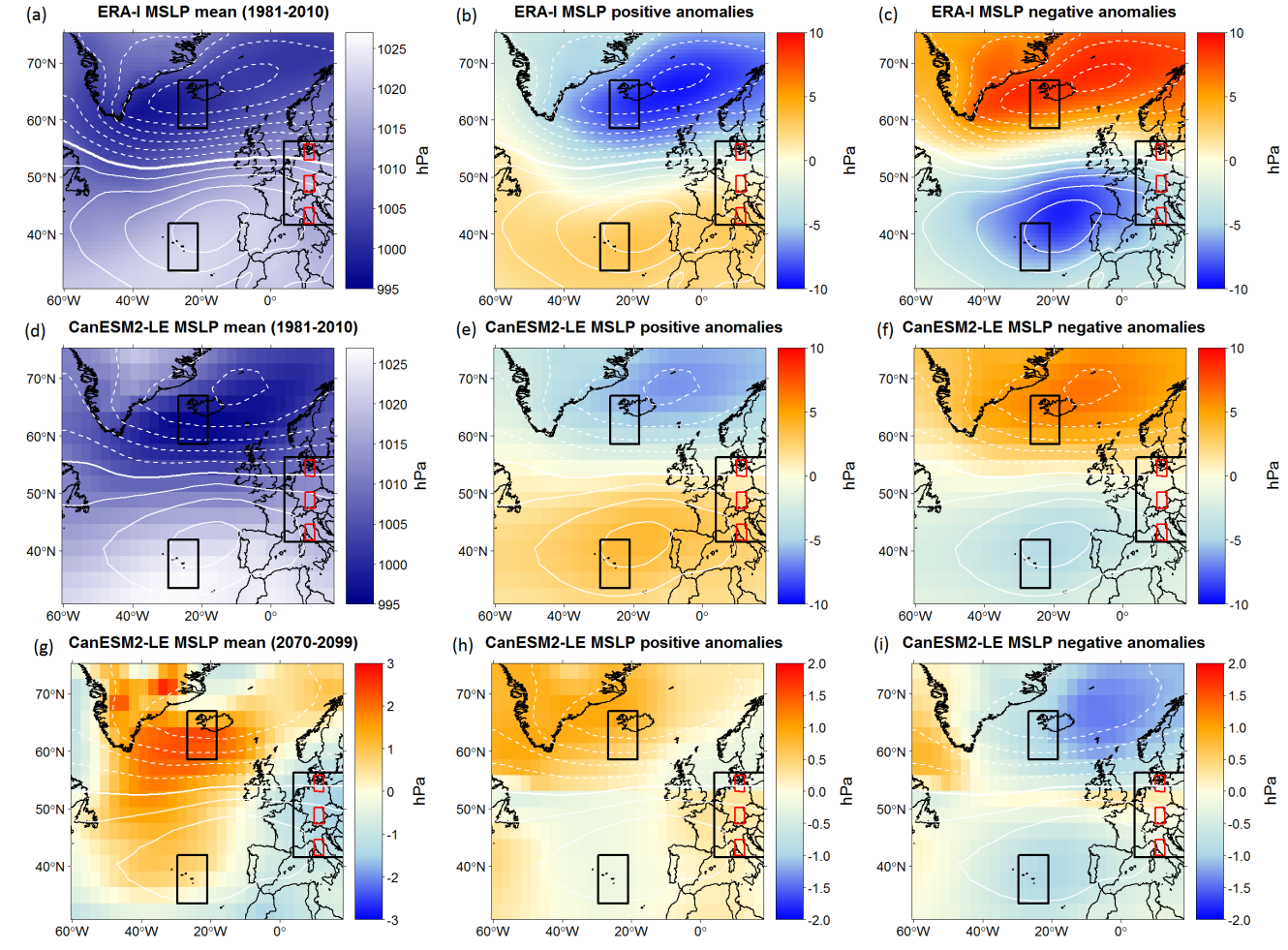

Figure 2. Winter mean sea level pressure (MSLP) [hPa] for REF ((a)–(c)) and GCM ((d)–(f)) composites (1981–2010) showing long-term average conditions (left), positive (mid) and negative anomalies (right) over the North Atlantic region. (g)–(i): 2070–2099 changes towards 1981–2010 in GCM data. White isolines: difference between positive and negative (dashed) anomalies by a step of 2.50 hPa, as e.g. in Hurrell (1995). Black boxes: regions used for index calculation over the North Atlantic and response region in central Europe. Red boxes: position of subset regions in Fig. 7.

ERA-I. They are not systematically related to the ERA-I (the "reference") realization.

Typical spatial psl features in the NAR region are shown in Fig. 2 for average, positive and negative NAO conditions. Positive and negative index years are chosen, if the respective absolute index value exceeds 1 as in Rogers (1984). This stratifies the original data in three subsets with positive, negative and indifferent index values. Under average psl conditions, the North
215 Atlantic region is characterized by a pressure dipole. This structure is intensified and tilted clockwise in the CanESM2-LE ensemble mean (middle row) compared to REF (top row). The difference between the CanESM2-LE mean and REF reaches

https://doi.org/10.5194/esd-2019-58
Preprint. Discussion started: 2 October 2019


Earth System Dynamics Discussions

up to 10 hPa in both directions, with the strongest overestimation above Greenland and underestimation over the North Sea. The multi-member composites of positive and negative phases also show less pronounced psl anomalies than the REF data. The difference between psl anomalies in positive and negative years representing the pressure variability is indicated by white lines. It is weaker in the CanESM2-LE mean than in ERA-I data, but located in similar regions. These NAO centres of action reach GCM (REF) psl differences between positive and negative conditions of about 12.5 (17.5) hPa in the IL region and 7.5 (10.0) hPa in the AH region. They do not coincide with the highest and lowest average psl values, but are situated near the 3×3 pixel grid matrices used for index calculation. This is very promising as it backs the choice of these psl centres for index calculation.

Under projected future climate conditions, psl rises over large parts of the North Atlantic and shows less variability (see Fig. 2 (g)–(i)). Future positive phases tend to be weaker as psl shows a marked increase in the northern NAO node region. Negative phases exhibit psl decreases in both node regions, although with larger changes in the northern region, resulting in negative phases to become slightly weaker as well.

3.1.2 Local climate response to the NAO

NAO tas and pr spatial responses as revealed in the ERA-I data are reproduced in their general properties under current climate conditions in the CanESM2-LE and CRCM5-LE (see Figs. 3, 4, 5). Strongest responses occur in the CRCM5/ERA-I run for all variables. Positive NAO conditions are accompanied by winters with warmer temperatures (up to $+2$ K per unit index change, see Fig. 3) and less day-to-day tas variability (see Fig. 5).

The generally positive relationship between tas mean and NAO (see Fig. 3) is strongest in the eastern parts of the domain. Regionally, the NAO explains up to 40–60 $\%$ of tas mean variability (see also Fig. A2 where the tas mean α_1 share of the entire winter standard deviation of daily temperature values is shown). Explained variance is highest in the CRCM5/ERA-I run and lowest in the CanESM2-LE. The reduction of tas variability reaches up to 0.4–0.6 K in the northern continental section while it is near zero in the southern part of the domain. In Fig. 5, the spatial patterns of ERA-I and CRCM5/ERA-I differ stronger than in Fig. 3, but CRCM5/ERA-I and LE mean agree well.

Positive phases are also accompanied by more humid conditions in the north (because of more pr), and drier conditions in the south of the CEUR domain (because of less pr, see Fig. 4). The strength of the NAO–pr relationship, r, is not affected by topography in any of the models within the domain; only the pivotal line crossing Europe is following the Alpine ridges. The change between positive and negative r and α_1 occurs within a very narrow region. Within the CanESM2-LE, this zero-line is shifted northwards compared to ERA-I, CRCM5/ERA-I and CRCM5-LE. As is visible in Fig. 4, higher α_1 values in mountainous regions indicate strong responses to NAO with orography. Regionally, the NAO accounts for 40–50 $\%$ of total pr sum variance, in both positively and negatively correlated regions. In the CRCM5-LE, single spots in mountainous regions (e.g., in the Dinaric Alps) show extremely high pr sum α_1 values (up to ± 220 mm per unit index change), stressing the more detailed production of geographical features in the RCM (see similar results for local daily extreme precipitation in Leduc et al., 2019). Pr sum shows only weak correlations and changes in the central region of the CEUR domain.

https://doi.org/10.5194/esd-2019-58
Preprint. Discussion started: 2 October 2019

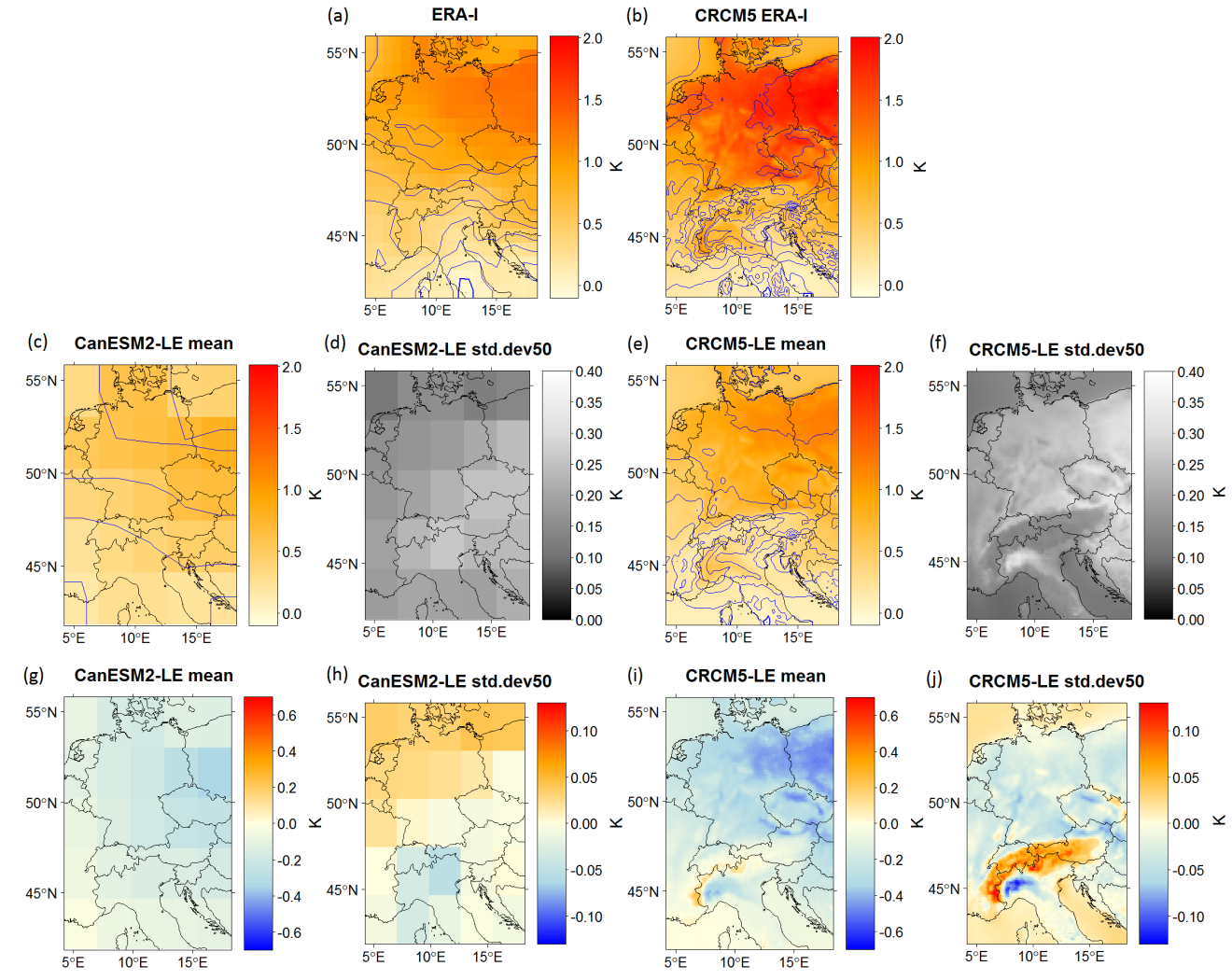

Figure 3. Spatial patterns of change in tas mean (in [K]) for a unit change in the NAO index for ERA-I, CRCM5/ERA-I, CanESM2-LE and CRCM5-LE in 1981–2010 ((a)–(f)) and the difference to 2070–2099 ((g)–(j)). Both 50-member ensembles are represented with ensemble mean and std.dev50. Blue isolines show the respective correlations by an increment of 0.1 (thick line is zero-correlation, solid lines positive).

The mean state of tas and pr changes in the transient climate simulation towards warmer and moister conditions with less intra-seasonal variability of tas. For a detailed description of the future climate evolution (though for 2080–2099) in Europe within the CRCM5-LE see Leduc et al. (2019). Future correlations weaken in general compared to the historical ones (apart from some regions in the south with increasing r for pr) for all variables which adds more noise to the signal: the signal-to-noise ratio (SNR) between LE ensemble means and std.dev50 is reduced for both CRCM5-LE and CanESM2-LE for tas and pr in the future period (see Fig. A3 and A4). This finding is valid for r and α_1. Less variance of tas and pr is explained by the NAO

https://doi.org/10.5194/esd-2019-58
Preprint. Discussion started: 2 October 2019

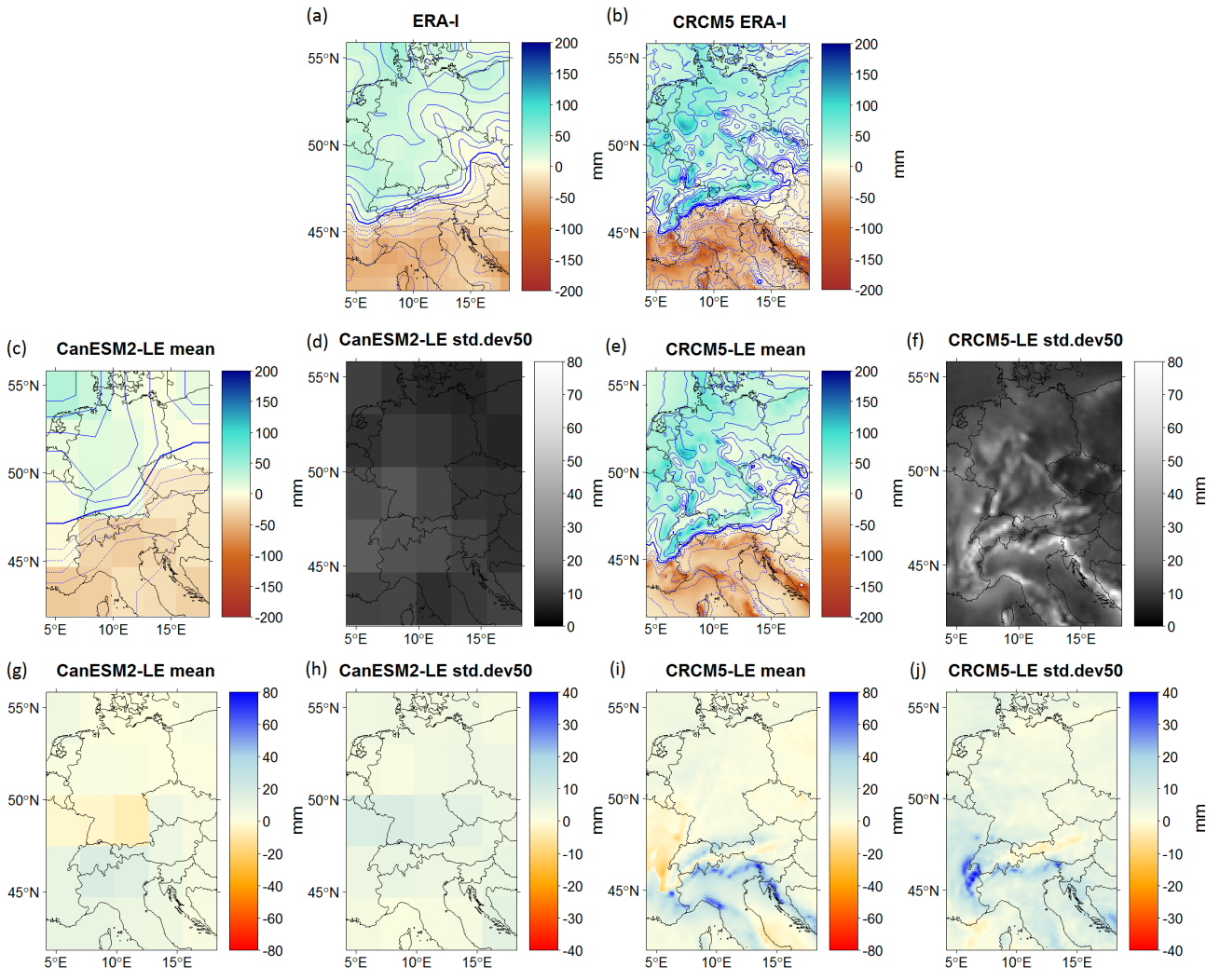

Figure 4. Spatial patterns of distributed change in pr sum (in [mm]) for a unit index change in the NAO index for ERA-I, CRCM5/ERA-I, CanESM2-LE and CRCM5-LE in 1981–2010 ((a)–(f)) and the difference to 2070–2099 ((g)–(j)). Both 50-member ensembles are represented with ensemble mean and std.dev50. Blue isolines show the respective correlations by an increment of 0.1 (thick line is zero-correlation, solid lines positive, dashed lines negative correlations). Note that the colour bar in the bottom row is flipped compared to Fig. 3.

(see α_1 distribution in Fig. 3 and Fig. 4, as well as Fig. A2 for tas mean). Also, tas std decreases less with unit index change in the projected future climate (Fig. 5 (g), (i), blue shading).

The spatial patterns of NAO-induced change though do not change considerably. The response to NAO impulses, α_1, is clearly reduced in tas mean as is tas std, and there is also a reduction in pr sum change.

https://doi.org/10.5194/esd-2019-58
Preprint. Discussion started: 2 October 2019

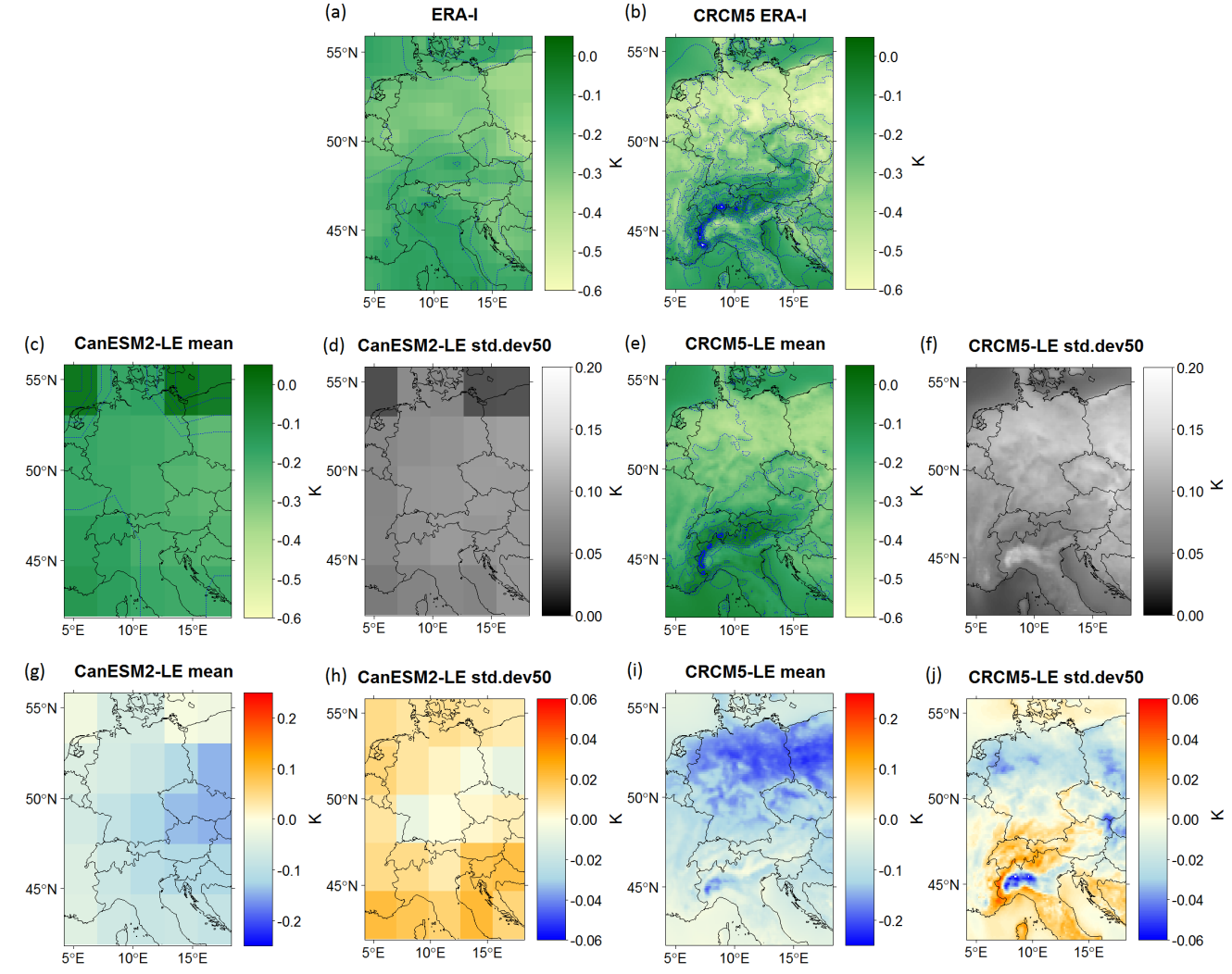

Figure 5. Spatial patterns of distributed change in tas std (in [K]) for a unit index change in the NAO index for ERA-I, CRCM5/ERA-I, CanESM2-LE and CRCM5-LE in 1981–2010 ((a)–(f)) and the difference to 2070–2099 ((g)–(j)). Both 50-member ensembles are represented with ensemble mean and std.dev50. Blue isolines show the respective correlations by an increment of 0.1 (thick line is zero-correlation, solid lines positive, dashed lines negative correlations). Note that the difference maps for CanESM2-LE and CRCM5-LE mean were calculated using absolute values.

3.2 Transferring Internal Variability from the GCM to the RCM scale

The transfer of internal variability from the GCM to the RCM is assessed via the difference in the inter-member spread of the CRCM5-LE compared to the CanESM2-LE.

265

https://doi.org/10.5194/esd-2019-58
Preprint. Discussion started: 2 October 2019

Earth System Dynamics
Discussions
Open Access
EGU

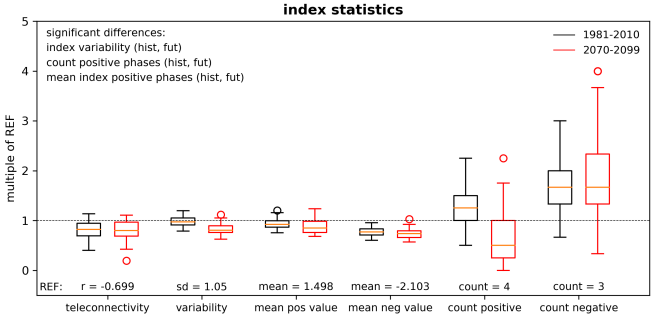

Figure 6. Several index statistics of all 50 CanESM2-LE members expressed as multiples of the respective ERA-I value (REF value set to 1.0): teleconnectivity (correlation between AH and IL time series), index variability (expressed as sd of index time series), mean value of all positive (negative) phases, count of all positive (negative) phases in a single realization. Positive (negative) years are defined by an absolute index value exceeding 1. Text in upper left corner: significantly ($p \leq 0.05$, using an unpaired Mann-Whitney/U-test) different outcomes in the future.

3.2.1 Multi-member ensemble

The CanESM2-LE reproduces typical index characteristics: Fig. 6 summarizes several statistics for all 50 GCM members as multiples of the REF value. Generally, the ensemble meets the REF value in all aspects of the NAO index. However, some GCM members only reach half of the REF teleconnectivity values (minimum: $r = -0.281$, not significant at $p \leq 0.05$; REF $r = -0.699$). This finding is especially interesting as this metric quantifies the strength of the NAO within the individual members. Internal variability of index characteristics is prone to significant changes between present and future conditions as is also seen in Fig. 6. The ensemble spread of the teleconnection strength, though, does not change significantly over time, in spite of the psl changes over the North Atlantic. The 2070–2099 NAO index exhibits less positive phases, more indifferent phases and thus a relative increase of negative phases but with reduced mean values (see also Fig. 1 (a)).

The spatial expression of NAO response internal variability in the form of diverging ensemble members can be derived from Figs. 3, 4, 5 (subplots (d), (f)) presenting spatially distributed std.dev50. Largest deviations for tas mean are found in continental regions of CEUR, but they do not generally correspond to high or low α_1. Low std.dev50 corresponds to Alpine and sea regions. For tas mean, the SNRs between ensemble mean and inter-member spread exceed 1 in most regions north of the Alps (see Fig. A3). Regarding pr sum, RCM members vary most in regions with highest absolute α_1 values and altitudes, while high α_1 of tas std are accompanied with large inter-member spreads for GCM and RCM. For pr sum, there is an east-west corridor of SNR values below 1 which accompanies rather low correlation values (see Fig. A4). This indicates that low ensemble average correlations in this region are mostly due to diverging correlation values among the single members (noise). The SNR shows similar spatial distributions in r and α_1 for tas mean and pr sum. In addition to future changes in the NAO responses means, there is also a change in the spatial distribution of the std.dev50 values (see Figs. 3, 4, 5, (h), (i)).

Figure 7 illustrates the inter-member spread in the spatially averaged subset regions for r between the NAO index and tas mean

https://doi.org/10.5194/esd-2019-58
Preprint. Discussion started: 2 October 2019

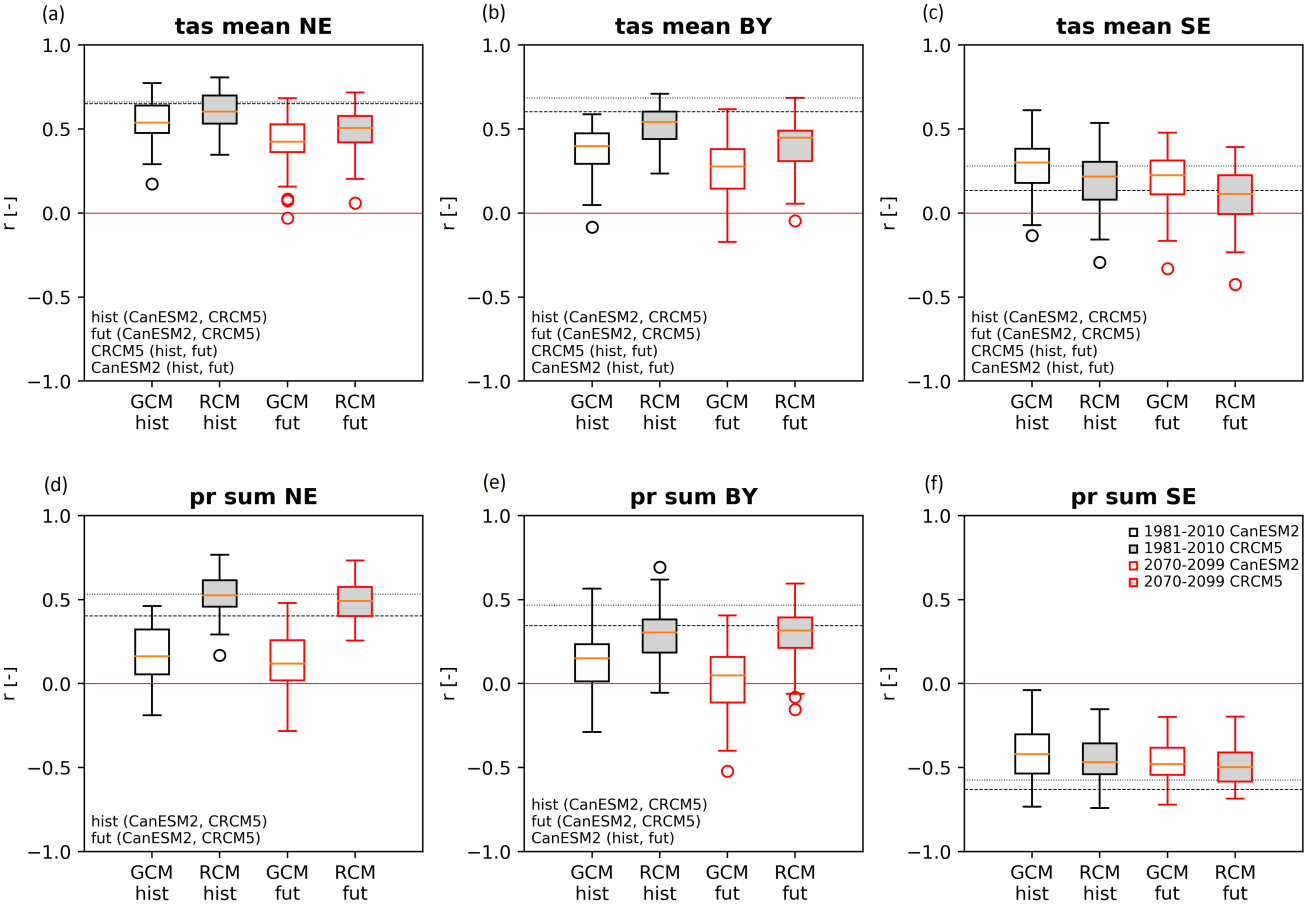

Figure 7. Boxplots of tas mean ((a)–(c)) and pr sum ((d)–(f)) showing r of 50 CanESM2-LE and CRCM5-LE (grey filling) realizations for three regions (NE, BY, SE) in historical (black outlines) and future (red outlines) time horizons. Dashed (dotted) horizontal lines indicate the ERA-I REF (CRCM5/ERA-I) value; text denotes combinations of which the differences are significant with $p \leq 0.05$ using an unpaired Mann-Whitney/U-test.

or pr sum. Both ensembles generally envelope the REF value (dashed line) of the given region, apart from GCM hist in tas BY. This finding does not change in the projected future climate: most boxes and whiskers keep their size, though pr SE (GCM) is characterized by a smaller range in the future (significant at $p \leq 0.10$ using an F-test for comparison of variances) and tas NE (GCM) by a larger one ($p \leq 0.05$, F-test). The (sometimes significant at $p \leq 0.05$, using an unpaired Mann-Whitney/U-test) shift of boxes towards lower r values in the future for both models is clearly visible for tas mean and pr sum.

https://doi.org/10.5194/esd-2019-58
Preprint. Discussion started: 2 October 2019

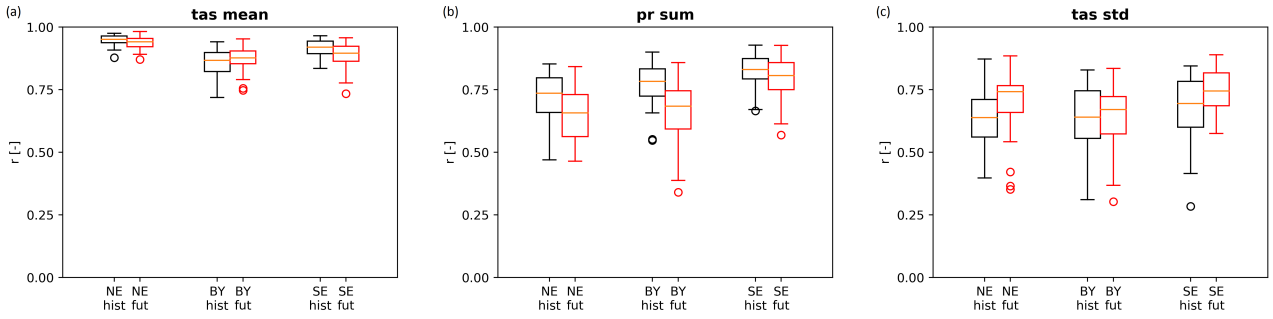

Figure 8. Similarity of matching CanESM2 and CRCM5 subset region (NE, BY, SE) time series (tas mean, pr sum) expressed as boxplots of r between matching GCM and RCM members. Hist: 1981–2010, fut: 2070–2099.

3.2.2 Change of scales

The amount of variance explained by the NAO is generally higher in REF than in the RCM ensemble mean, which in turn is higher than the GCM ensemble mean. The CRCM5-LE enhances the relationship showing higher r and α_1 values than the CanESM2-LE (see Fig. 7 for r, where hist(CanESM2, CRCM5) or fut(CanESM2, CRCM5) is indicated; but also Figs. 3, 4 and 5). This enhancement by the CRCM5 is notable independent of the driving data: for both variables, the CRCM5/ERA-I r value (dotted lines in Fig. 7) is also found to be higher than the ERA-I value in most regions (dashed lines in Fig. 7; see also Fig. A5, first column, for spatial distribution of the CRCM5/ERA-I error). In all subset regions, the CRCM5/ERA-I r value lies in the upper part (stronger correlations) of the CRCM5-LE ensemble values.

Figure 7 shows that mean r values of RCM (grey filling) and GCM (hollow) members are significantly different in all subset regions for tas mean in both time horizons, but only in the NE and BY regions for pr sum; in SE, effectively no difference between GCM and RCM pr sum r distributions is visible. Apart from pr NE (both time horizons) no significant (at $p \leq 0.05$, F-test) box size (spread amplitude) difference between GCM and RCM is visible. In NE and BY this difference is expressed by higher r values in RCM data, whereas in the SE region lower r values are found in the RCM data (only for tas mean). Thus the inter-member spread of the correlation between NAO and response variables is not generally altered during the nesting process.

When correlating matching subset region time series (see Fyfe et al., 2017, for a similar approach) of CanESM2-LE and CRCM5-LE as in Fig. 8, highest accordance on average is reached for tas mean, indicating that CanESM2-LE and CRCM5-LE show very similar temporal variability for this variable. The correlations between CanESM2 and CRCM5 subset regions are in general significantly lower under future climate conditions. The accordance of pr sum and tas std are weaker than for tas mean in both time frames.

https://doi.org/10.5194/esd-2019-58
Preprint. Discussion started: 2 October 2019

Earth System Dynamics Discussions

4 Discussion

The ClimEx climate data ensemble is able to reproduce an NAO-like pattern with realistic temporal and spatial characteristics over the North Atlantic and corresponding response patterns in CEUR. Coincidentally, the index derived from one realization shows a very strong temporal correlation with the REF NAO index (see Fig. A6, first and second row).

The strong psl gradient suggests an overestimation of the local atmospheric circulation with too strong westerlies over the North Atlantic in the background state within the CanESM2-LE. Similar model biases are widely reported (see e.g. Ruprich-Robert and Cassou, 2015; Stephenson et al., 2006; Reintges et al., 2017; Ulbrich et al., 2008). Positive and negative NAO states appear to be weaker within the CanESM2-LE. This difference between GCM and REF is possibly due to the fact that REF composites were derived from 3 negative and 4 positive years whereas the GCM data provided 264 negative and 263 positive years. The GCM patterns are thus more robustly assessed (that is, less prone to incidental fluctuations of single realizations).

Concerning NAO responses, they are most reliable in regions where r is significant (i.e. $|r| > 0.361$ for $p \leq 0.05$, corresponding to a coefficient of determination $r^2 = 0.130$ or 13 % of tas/pr variance explained by the NAO). On the other hand, lower correlation values ($|r| < 0.361$) suggest that climate variability at the local scale evolves differently from the global teleconnection. In these cases, the NAO is not the most important contributor and ε_Y in Eq. (2) is dominant. Since the index was obtained from raw psl data, it contains the NAO contribution, but possibly also of other teleconnection patterns and noise.

Historical α_1 values (all data sources) are generally in accordance with composite anomalies (see also Fig. A1), but most so in regions with significant r. Thus, the future change of tas and pr per unit index change is most valid where r is significant and where the signals of α_1 and r emerge from the internal noise, i.e. the SNR is larger than 1. Of course, α_1 and composite maps are not identical, as on the one hand the mean index value that accompanies tas and pr anomalies is not the same (± 1 for α_1, but $+1.498$ and -2.103 for REF composites, see Fig. 6). On the other hand, α_1 estimates a change which is singularly generated by the NAO, while composite maps originate from raw data which might include further influences (Eq. (2)).

Regarding temperature, Europe is commonly seen as divided into a region with positive NAO–response correlations in the north and negative correlations in the south (see e.g., Woollings et al., 2015). The first is found in the here presented results, the latter is not as clear in the chosen domain. Strong correlations of pr sums and NAO are in accordance with the prevalence of large-scale (frontal) precipitation in winter, which might be affected if the large-scale circulation is altered due to NAO impulses. The third variable, tas std, is correlated negatively with the NAO, pointing towards less temperature variability in winters with positive NAO phases, and a higher variability in negative phases. This also fits the observation of altered jet stream and storm track behaviour.

NAO response patterns are similar within the CanESM2-LE and CRCM5-LE, but some deviations remain due to differences in model parameterization and spatial resolution. Another possible explanation could be that the control exerted by CanESM2 through the CRCM5 lateral boundary conditions (LBC) is insufficient, but this is unlikely given the relatively small CRCM5 domain implying stronger LBC control (Leduc and Laprise, 2009), in addition to the strong spectral nudging of large scales that was applied in the production of the CRCM5-LE (Leduc et al., 2019). The CRCM5 reproduces the structure found in ERA-I much finer than the CanESM2 and adds some high resolution geographical features which are clearly visible within the

https://doi.org/10.5194/esd-2019-58
Preprint. Discussion started: 2 October 2019

ensemble mean.

Typical continental climate features, such as higher tas variability (as indicated by Fig. 3), are shifted southwards in the CanESM2-LE with respect to CRCM5-LE data (or ERA-I). This may be explained by the fact that due to coarser spatial resolution the GCM topography shows land grid cells where the Mediterranean extends in ERA-I and CRCM5; thus, in the GCM, the continent Europe also occupies a region, which is sea in ERA-I. Assuming that the land–sea distribution affects the climate evolution, the GCM also experiences a geographical shift of climatic characteristics (such as continental properties) compared with the ERA-I data. This in turn suggests that similar responses of GCM and RCM to the NAO may not be visible at the same geographical location (i.e., coordinates), but under similar geographical conditions (altitude, distance to sea).

As mentioned previously, the correlations in the CRCM5 are significantly stronger in several regions than in the CanESM2. These are not evened out by spatial aggregation (see Fig. 7) and the weaker correlations in CanESM2-LE mean cannot be related to a larger inter-member spread in the CanESM2-LE in general (see Figs. 3, 4 and 5 (d), (f)). Thus, in the CRCM5-LE, more variance is explained by the NAO (i.e., by large-scale circulation) than in the CanESM2-LE. Figure A5 shows that the CRCM5 tends to underestimate (overestimate) average winter mean tas in the northern (southern) part of the domain, regardless of the driving data (see first column for ERA-I and third column for CanESM2), whereas winter pr sums are overestimated nearly in the entire domain with strongest values in the south-eastern part. The GCM is also found to overestimate temperature and precipitation in the entire domain.

On the other hand, explained variance is higher in ERA-I and CRCM5/ERA-I than in the ensemble mean of GCM and RCM. Interestingly, Stephenson et al. (2006), who worked on a multi-model ensemble (with each model represented by a single member), noted a tendency for overestimation of explained variance regarding temperature and precipitation compared to observations in all of their models.

The large ensemble internal variability favours a smoothing of structures in the ensemble average. However, as the ensemble mean (GCM and RCM) reproduces patterns very similar to the observed ones, the atmospheric dynamics behind are correctly incorporated in all members: each pattern, as given by a single member, may occur as a response to the NAO, even if it deviates strongly from the observed patterns.

In general, the 50 NAO signals from the atmospheric "inflow" as given by the GCM boundary conditions are correctly translated into 50 regional responses of the RCM regarding the range of internal variability.

The amplitude of the inter-member spread of r is similar in RCM and GCM. Thus, the range of internal variability regarding the strength of the NAO–response relationship is transferred during nesting and the CRCM5 added internal variability (Leduc et al., 2019) does not significantly alter it. However, the spread is shifted towards higher r values in the RCM compared to the GCM. Similar results are found when comparing present and future values: a vertical shift of the boxes in Fig. 7 indicates that r is reduced in the future, but the inter-quartile distance of the r distributions (box size) stays nearly the same.

The REF time series fits the ensemble statistics and may therefore be seen as a realization out of the ensemble. In other words, it can be argued that the ensemble and the REF time series represent the same climate statistics. The ensemble thus produces NAO and response patterns that are more robust than patterns of single realizations.

Further on, the std.dev50 maps in Figs. 3, 4 and 5 show that the deviation of tas mean, tas std and pr sum α_1 also have a

https://doi.org/10.5194/esd-2019-58
Preprint. Discussion started: 2 October 2019

spatial dimension: generally, this deviation is strongest in regions with highest change in CRCM5-LE, but not automatically in CanESM2-LE.

The NAO index variability is reduced in the future climate simulation at the same time as tas variability. This reduction is accompanied by a higher inter-member spread of α_1. The relative prevalence of negative index phases occurs in correspondence to a generally strengthened high pressure ridge over the North Atlantic and especially Greenland (see Fig. 2 (g)). The latter feature is supposed to foster negative index phases (Hanna et al., 2015; Benedict et al., 2004). An increasing frequency (relative to positive phases) of negative NAO events as noted in Fig. 1 favours more cold and harsh winters in theory which is in great contradiction to the future background conditions (warmer, moister, see Leduc et al., 2019) that would rather, likewise following from theory, accompany positive phases. On the other hand, the response to NAO impulses is clearly reduced in tas mean, pr sum and tas std α_1. A coherent explication for this discrepancy might be that as correlations weaken, the Eurasian (continental) influence during negative phases may be repressed or weaker in its occurrence than now. As less tas and pr variance is explained by the NAO in the future climate projections, the influence of this climate mode on CEUR climate is reduced.

5 Conclusions

Both large ensembles within the ClimEx project climate model chain are able to depict a robust, realistic NAO pattern under current forcing conditions, although the NAO structure itself evolves outside the analyzed CEUR domain (key question (a)). Each member represents a distinct climate evolution while sharing comparable statistics with all other 49 realizations. The clearly visible connection of the NAO with tas mean and pr sum follows well-known patterns, but also the influence on tas variability, as expressed by the analyses on tas std, is remarkable.

Internal variability of the NAO pattern is expressed very well within the 50 member single-model ensemble, and easily spans the observations regarding various indicators, like the strength of the teleconnection or the temporal variability of the index time series in a 30 year period. The range of NAO responses is transferred correctly from the driving GCM into the nested RCM. The spread is shifted towards stronger NAO–tas/pr relations in the RCM compared to the GCM in both time horizons. Clearly more topographic features are visible in the CRCM5-LE than in the CanESM2-LE which proves the added value of RCM regarding the evaluation of regional NAO impacts. Deviations of NAO tas and pr responses between members vary spatially within the domain and are found mostly in regions with strongest NAO responses (key questions (b), (c)).

Concerning climate change (key question (d)), several changes go hand in hand: the winter index variability is reduced, the overall winter variability of tas and pr and also the fraction of NAO-explained tas is reduced, the relationship between NAO and climate is weakened and the co-variability of CanESM2 and CRCM5 subset regions for all weather variables is reduced.

While these results are especially valid for the ClimEx data sets, they allow drawing some general conclusions. The results strengthen the validity of the climate module for further applications, as important large-scale teleconnections only present in the GCM propagate properly to the fine scale dynamics in the RCM. Thus the RCM does not alter the spread of driving GCM data which is a valuable information for impact modelling with a focus on internal variability. The results also stress the impor-

https://doi.org/10.5194/esd-2019-58
Preprint. Discussion started: 2 October 2019


Earth System Dynamics Discussions
Open Access
EGU

tance of single-model ensembles for evaluating and estimating internal variability since single realizations show considerable variations among themselves and also deviations from the ensemble mean. So the ensemble mean and the ensemble spread together are needed for robust assessment of climate modes and whether a given model is able to reproduce the phenomenon of interest.

Data availability. Data used in this study may be retrieved from the following sources:
CanESM2-LE data is available via http://collaboration.cmc.ec.gc.ca/cmc/cccma/CanSISE/output/CCCma/CanESM2/
CRCM5-LE data can be retrieved at https://climex-data.srv.lrz.de/Public/
ERA-Interim Reanalysis data set was obtained at https://apps.ecmwf.int/datasets/data/interim-full-daily/levtype=sfc/

Appendix A

https://doi.org/10.5194/esd-2019-58
Preprint. Discussion started: 2 October 2019

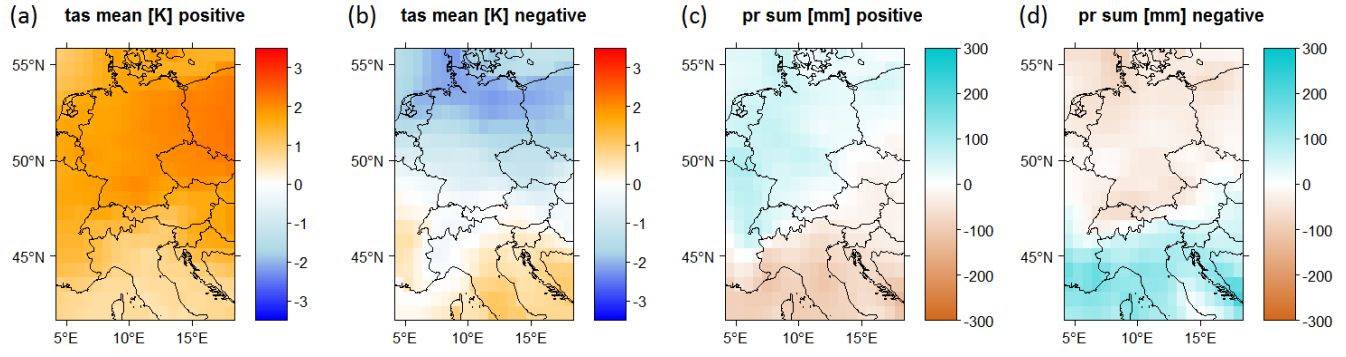

Figure A1. ERA-I anomalies from the long-term mean of tas mean in [K] and pr sum in [mm] in NAO positive (1989, 1990, 1994, 1995) and negative (1996, 2001, 2010) winters. Mean index value for positive (negative) NAO phases is $+1.498$ (-2.103).

https://doi.org/10.5194/esd-2019-58
Preprint. Discussion started: 2 October 2019

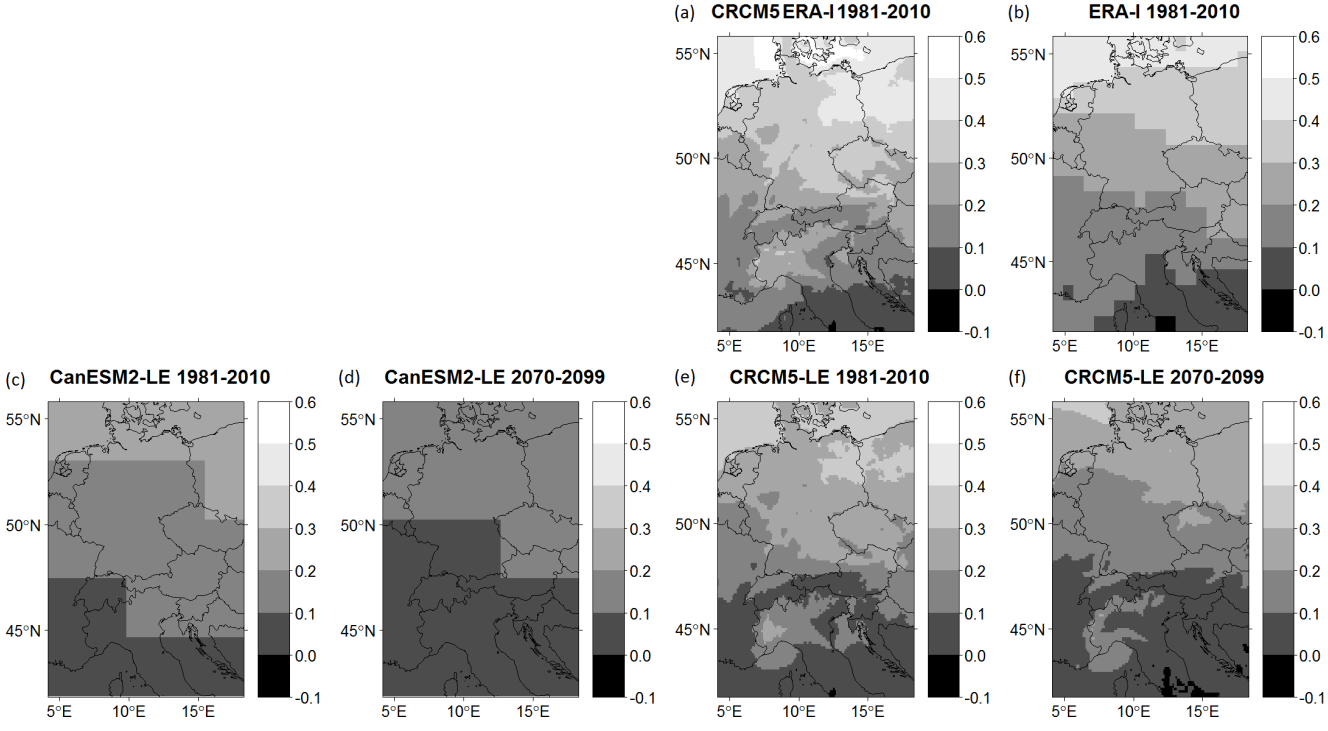

Figure A2. Ratio of tas α_1 and winter mean daily standard deviation of tas.

https://doi.org/10.5194/esd-2019-58
Preprint. Discussion started: 2 October 2019

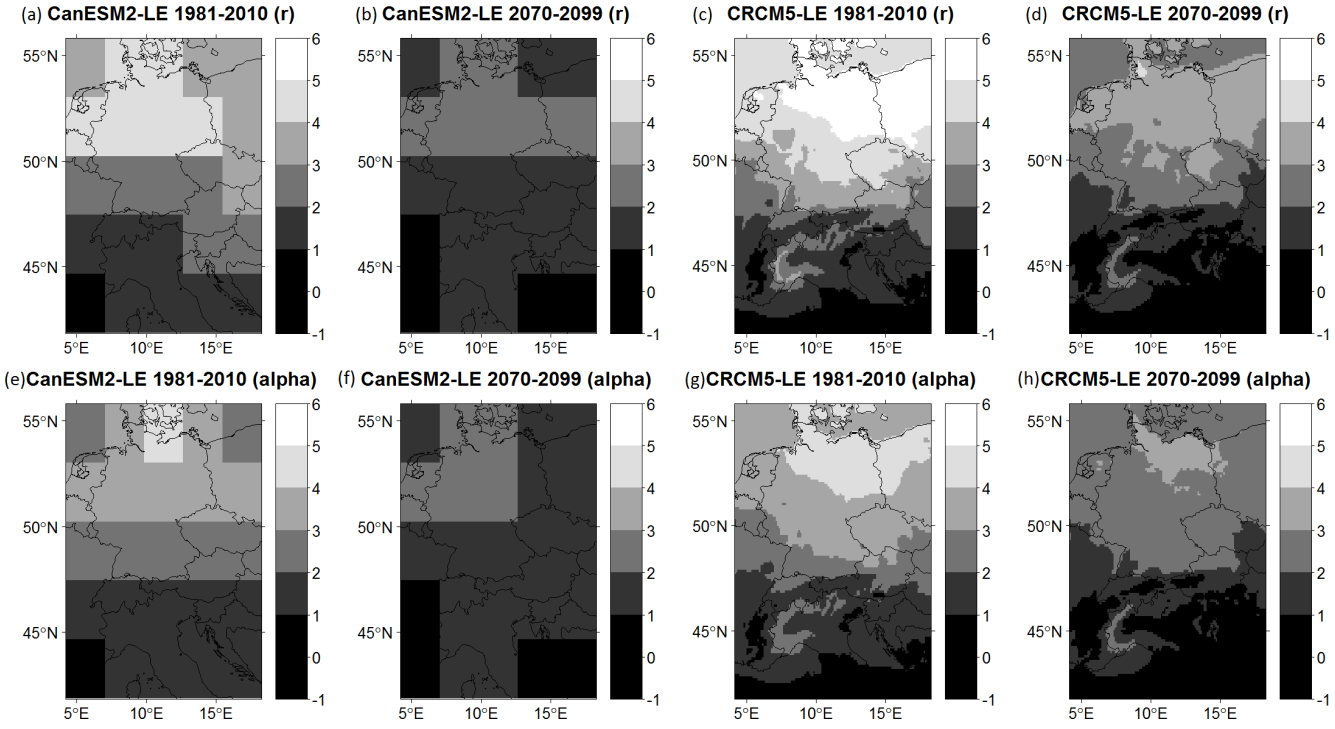

Figure A3. Signal to noise ratio (SNR) between ensemble mean and std.dev50 for tas mean: Pearson correlation coefficient ((a)–(d)) and α_1 value ((e)–(h)). Black: regions with SNR $< |1|$. Negative values emerging due to negative r and α_1 values.

https://doi.org/10.5194/esd-2019-58
Preprint. Discussion started: 2 October 2019

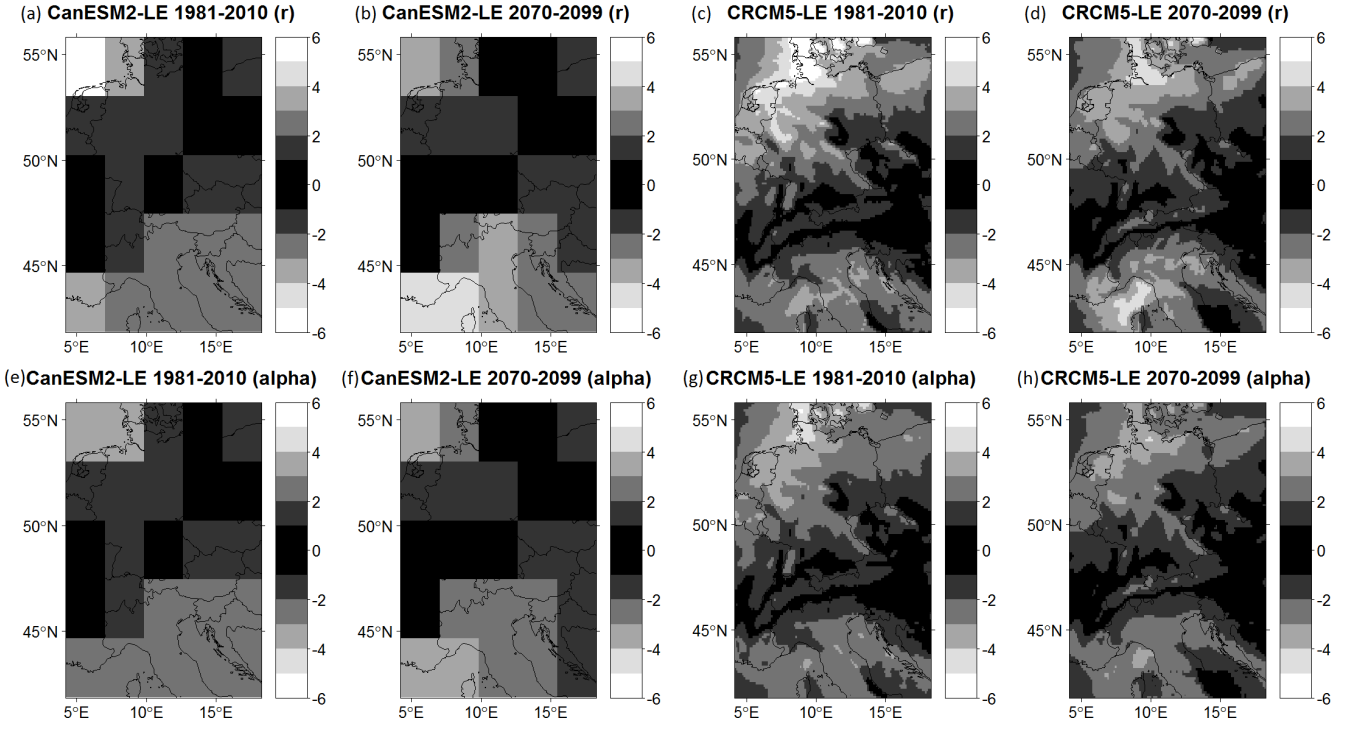

Figure A4. Signal to noise ratio (SNR) between ensemble mean and std.dev50 for pr sum: Pearson correlation coefficient ((a)–(d)) and α_1 value ((e)–(h)). Black: regions with SNR $< |1|$. Negative values emerging due to negative r and α_1 values. Usage of symmetric colour bar as only strength of SNR is of importance in this case.

https://doi.org/10.5194/esd-2019-58
Preprint. Discussion started: 2 October 2019

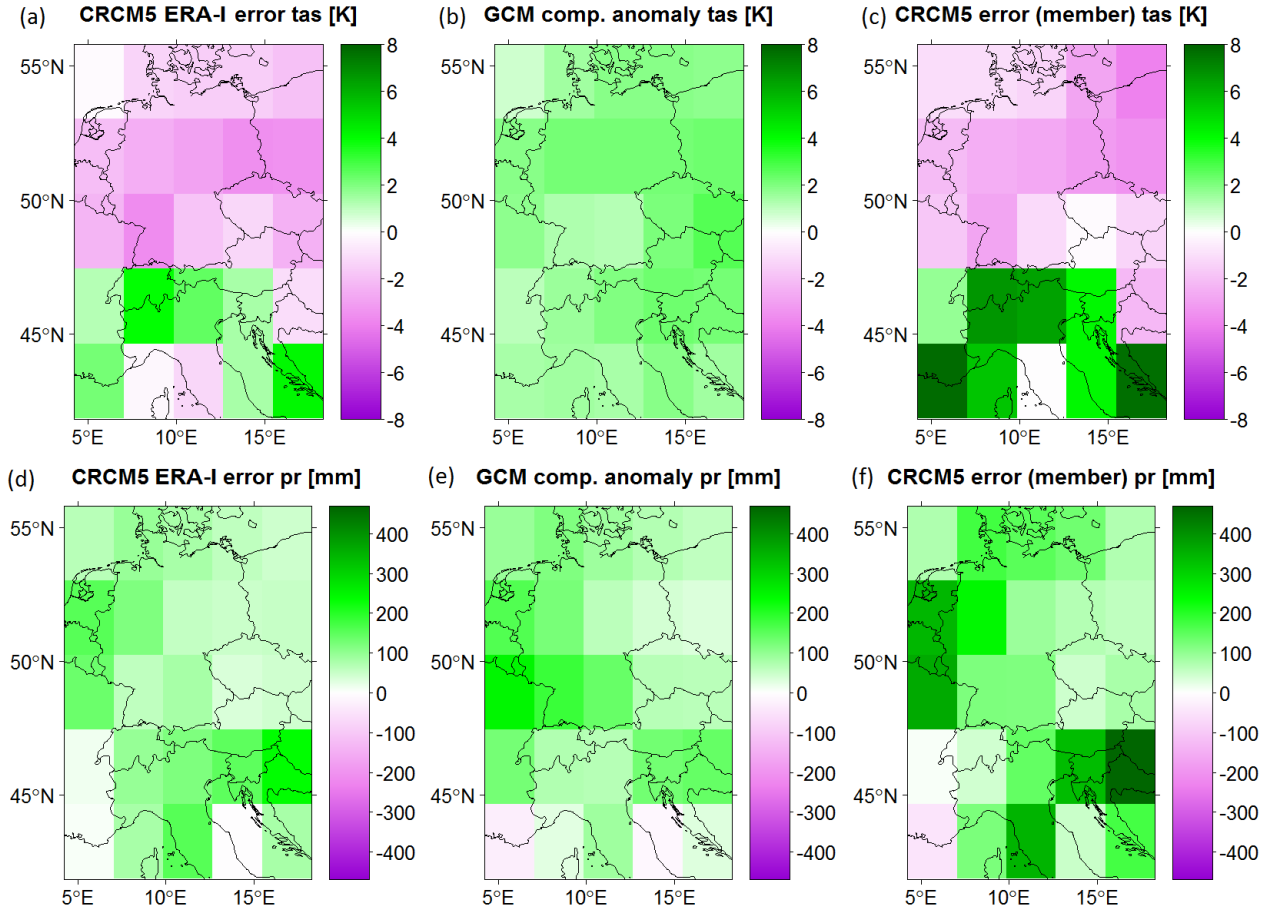

Figure A5. Model errors for 30 winter tas mean averages ((a)–(c)) and 30 winter pr sum averages ((d)–(f)) in GCM resolution (2.8°). First column: error of CRCM5 under "perfect"/ERA-I boundary conditions (difference between CRCM5/ERA-I and ERA-I). Second column: anomaly of GCM component of RCM towards ERA-I data (ensemble average of differences between GCM component of RCM and ERA-I). Third column: CRCM5 error under GCM boundary conditions (ensemble average of differences between CRCM5 members and corresponding CanESM2 members).

https://doi.org/10.5194/esd-2019-58
Preprint. Discussion started: 2 October 2019

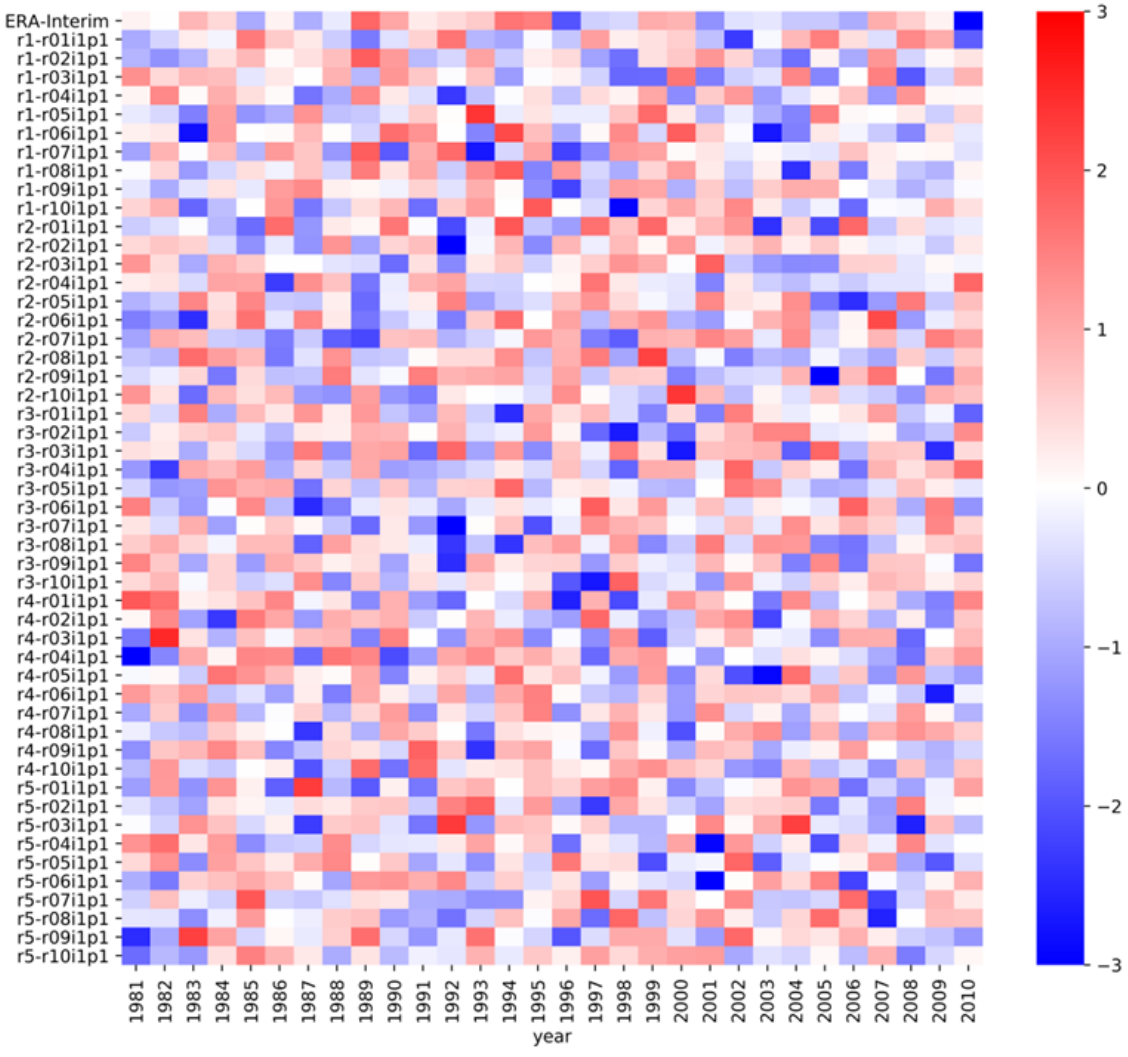

Figure A6. NAO index time series for all 50 CanESM2 members (see row names on the left side) for 1981–2010. The first row presents the reference (ERA-I) time series. Colour: winter index values of single years.

https://doi.org/10.5194/esd-2019-58
Preprint. Discussion started: 2 October 2019

Earth System Dynamics Discussions

Author contributions. This study was conceptualized by AB under supervision of RL. Formal analysis, visualization of results and writing of the original draft was performed by AB. All authors contributed to the interpretation of the findings and revision of the paper.

Competing interests. The authors declare that they have no competing interests.

Acknowledgements. The production of ClimEx was funded within the ClimEx project by the Bavarian State Ministry for the Environment and Consumer Protection. The CRCM5 was developed by the ESCER centre of Université du Québec à Montréal (UQAM; www.escer.uqam.ca) in collaboration with Environment and Climate Change Canada. We acknowledge Environment and Climate Change Canada's Canadian Centre for Climate Modelling and Analysis for executing and making available the CanESM2 Large Ensemble simulations used in this study, and the Canadian Sea Ice and Snow Evolution Network for proposing the simulations. Computations with the CRCM5 for the ClimEx project were made on the SuperMUC supercomputer at Leibniz Supercomputing Centre (LRZ) of the Bavarian Academy of Sciences and Humanities. The operation of this supercomputer is funded via the Gauss Centre for Supercomputing (GCS) by the German Federal Ministry of Education and Research and the Bavarian State Ministry of Education, Science and the Arts.

https://doi.org/10.5194/esd-2019-58
Preprint. Discussion started: 2 October 2019

Earth System Dynamics Discussions

References

Benedict, J., Lee, S., and Feldstein, S.: Synoptic View of the North Atlantic Oscillation, Journal of the Atmospheric Sciences, 61, 121–144, https://doi.org/10.1175/1520-0469(2004)061<0121:SVOTNA>2.0.CO;2, 2004.

Christensen, J., Krishna Kumar, K., Aldrian, E., An, S.-I., Cavalcanti, I., de Castro, M., Dong, W., Goswami, P., Hall, A., Kanyanga, J., Kitoh, A., Kossin, J., Lau, N.-C., Renwick, J., Stephenson, D., Xie, S.-P., and Zhou, T.: Climate Phenomena and their Relevance for Future Regional Climate Change, in: Climate Change 2013: The Physical Science Basis. Contribution of Working Group I to the Fifth Assessment Report of the Intergovernmental Panel on Climate Change, edited by Stocker, T., Qin, D., Plattner, G.-K., Tignor, M., Allen, S., Boschung, J., Nauels, A., Xia, Y., Bex, V., and Midgley, P., pp. 1271–1308, Cambridge University Press, Cambridge, United Kingdom and New York, USA, 2013.

Cropper, T., Hanna, E., Valente, M., and Jónsson, T.: A daily Azores-Iceland North Atlantic Oscillation index back to 1850, Geoscience Data Journal, 2, 12–24, https://doi.org/10.1002/gdj3.23, 2015.

Dee, D., Uppala, S., Simmons, A., Berrisford, P., Poli, P., Kobayashi, S., Andrae, U., Balmaseda, M., Balsamo, G., Bauer, P., Bechtold, P., Beljaars, A., van de Berg, L., Bidlot, J., Bormann, N., Delsol, C., Dragani, R., Fuentes, M., Geer, A., Haimberger, L., Healy, S., Hersbach, H., Hólm, E., Isaksen, L., Kållberg, P., Köhler, M., Matricardi, M., McNally, A., Monge-Sanz, B., Morcrette, J.-J., Park, B.-K., Peubey, C., de Rosnay, P., Tavolato, C., Thépaut, J.-N., and Vitart, F.: The ERA-Interim reanalysis: Configuration and performance of the data assimilation system, Quarterly Journal of the Royal Meteorological Society, 137, 553–597, https://doi.org/10.1002/qj.828, 2011.

Delworth, T., Zeng, F., Vecchi, G., Yang, X., Zhang, L., and Zhang, R.: The North Atlantic Oscillation as a driver of rapid climate change in the Northern Hemisphere, Nature Geoscience, 9, 509–512, https://doi.org/10.1038/ngeo2738, 2016.

Déqué, M., Rowell, D., Lüthi, D., Giorgi, F., Christensen, J., Rockel, B., Jacob, D., Kjellström, E., de Castro, M., and van den Hurk, B.: An intercomparison of regional climate simulations for Europe: assessing uncertainties in model projections, Climate Change, 81, 53–70, https://doi.org/10.1007/s10584-006-9228-x, 2007.

Deser, C., Phillips, A., Bourdette, V., and Teng, H.: Uncertainty in climate change projections: the role of internal variability, Climate Dynamics, 38, 527–546, https://doi.org/10.1007/s00382-010-0977-x, 2012.

Deser, C., Hurrell, J., and Phillips, A.: The role of the North Atlantic Oscillation in European climate projections, Climate Dynamics, 49, 3141–3157, https://doi.org/10.1007/s00382-016-3502-z, 2016.

Fyfe, J., Derksen, C., Mudryk, L., Flato, G., Santer, B., Swart, N., Molotch, N., Zhang, X., Wan, H., Arora, V., Scinocca, J., and Jiao, Y.: Large near-term projected snowpack loss over the western United States, Nature communications, 8, 1–7, https://doi.org/10.1038/ncomms14996, 2017.

Gillett, N. and Fyfe, J.: Annular mode changes in the CMIP5 simulations, Geophysical Research Letters, 40, 1189–1193, https://doi.org/10.1002/grl.50249, 2013.

Hanna, E., Cropper, T., Jones, P., Scaife, A., and Allan, R.: Recent seasonal asymmetric changes in the NAO (a marked summer decline and increased winter variability) and associated changes in the AO and Greenland Blocking Index, International Journal of Climatology, 35, 2540–2554, https://doi.org/10.1002/joc.4157, 2015.

Hansen, F., Greatbatch, R., Gollan, G., Jung, T., and Weisheimer, A.: Remote control of North Atlantic Oscillation predictability via the stratosphere, Quarterly Journal of the Royal Meteorological Society, 143, 706–719, https://doi.org/10.1002/qj.2958, 2017.

Hawkins, E. and Sutton, R.: The Potential To Narrow Uncertainty in Regional Climate Predictions, Bulletin of the American Meteorological Society, 90, 1095–1107, http://dx.doi.org/10.1175/2009bams2607.1, 2009.

https://doi.org/10.5194/esd-2019-58
Preprint. Discussion started: 2 October 2019

Hawkins, E. and Sutton, R.: The Potential To Narrow Uncertainty in Projections of Regional Precipitation Change, Climate Dynamics, 37, 407–418, http://dx.doi.org/10.1007/s00382-010-0810-6, 2011.

Hurrell, J. W.: Decadal Trends in the North Atlantic Oscillation: Regional Temperatures and Precipitation, Science, 269, 676–679, https://doi.org/10.1126/science.269.5224.676, 1995.

Hurrell, J. W. and Deser, C.: North Atlantic climate variability: The role of the North Atlantic Oscillation, Journal of Marine Systems, 78, 28–41, https://doi.org/10.1016/j.jmarsys.2009.11.002, 2009.

Hurrell, J. W. and Van Loon, H.: Decadal variations in climate associated with the North Atlantic Oscillation, Climatic Change, 36, 301–326, https://doi.org/10.1023/A:1005314315270, 1997.

Iles, C. and Hegerl, G.: Role of the North Atlantic Oscillation in decadal temperature trends, Environmental Research Letters, 12, 1–10, https://doi.org/10.1088/1748-9326/aa9152, 2017.

Jones, P., Osborn, T., and Briffa, K.: Pressure-Based Measures of the North Atlantic Oscillation (NAO): A Comparison and an Assessment of Changes in the Strength of the NAO and its Influence on Surface Climate Parameters, in: The North Atlantic Oscillation. Climatic Significance and Environmental Impact, edited by Hurrell, J., Kushnir, Y., Ottersen, G., and Visbeck, M., pp. 51–62, American Geophysical Union, Washington, D.C., https://doi.org/10.1029/134GM03, 2003.

Kirtman, B., Power, S., Adedoyin, J., Boer, G., Bojariu, R., Camilloni, I., Doblas-Reyes, F., Fiore, A., Kimoto, M., Meehl, G., Prather, M., Sarr, A., Schär, C., Sutton, R., van Oldenborgh, G., Vecchi, G., and Wang, H.: Near-term Climate Change: Projections and Predictability, in: Climate Change 2013: The Physical Science Basis. Contribution of Working Group I to the Fifth Assessment Report of the Intergovernmental Panel on Climate Change, edited by Stocker, T., Qin, D., Plattner, G.-K., Tignor, M., Allen, S., Boschung, J., Nauels, A., Xia, Y., Bex, V., and Midgley, P., pp. 953–1028, Cambridge University Press, Cambridge, United Kingdom and New York, USA, 2013.

Leduc, M. and Laprise, R.: Regional climate model sensitivity to domain size, Climate Dynamics, 32, 833–854, https://doi.org/10.1007/s00382-008-0400-z, 2009.

Leduc, M., Mailhot, A., Frigon, A., Martel, J.-L., Ludwig, R., Brietzke, G., Giguère, M., Brissette, F., Turcotte, R., Braun, M., and Scinocca, J.: The ClimEx Project: A 50-Member Ensemble of Climate Change Projections at 12-km Resolution over Europe and Northeastern North America with the Canadian Regional Climate Model (CRCM5), Journal of Applied Meteorology and Climatology, 58, 663–693, https://doi.org/10.1175/JAMC-D-18-0021.1, 2019.

Moore, G., Renfrew, I., and Pickart, R.: Multidecadal Mobility of the North Atlantic Oscillation, Journal of Climate, 26, 2453–2466, https://doi.org/10.1175/JCLI-D-12-00023.1, 2013.

Osborn, T.: Simulating the winter North Atlantic Oscillation: the roles of internal variability and greenhouse gas forcing, Climate Dynamics, 22, 605–623, https://doi.org/10.1007/s00382-004-0405-1, 2004.

Pokorná, L. and Huth, R.: Climate impacts of the NAO are sensitive to how the NAO is defined, Theoretical Applied Climatology, 119, 639–652, https://doi.org/10.1007/s00704-014-1116-0, 2015.

Reintges, A., Latif, M., and Park, W.: Sub-decadal North Atlantic Oscillation variability in observations and the Kiel Climate Model, Climate Dynamics, 48, 3475–3487, https://doi.org/10.1007/s00382-016-3279-0, 2017.

Rogers, J.: The Association between the North Atlantic Oscillation and the Southern Oscillation in the Northern Hemisphere, Monthly Weather Review, 112, 1999–2015, https://doi.org/10.1175/1520-0493(1984)112<1999:TABTNA>2.0.CO;2, 1984.

Ruprich-Robert, Y. and Cassou, C.: Combined influences of seasonal East Atlantic Pattern and North Atlantic Oscillation to excite Atlantic multidecadal variability in a climate model, Climate Dynamics, 44, 229–253, https://doi.org/10.1007/s00382-014-2176-7, 2015.

https://doi.org/10.5194/esd-2019-58
Preprint. Discussion started: 2 October 2019

Schulzweida, U.: CDO User Guide. Climate Data Operators Version 1.9.1. October 2017, MPI for Meteorology. URL: https://code.mpimet.mpg.de/projects/cdo/embedded/cdo.pdf., access: 01.04.2018, 2017.

Stephenson, D., Pavan, V., Collins, M., Junge, M., and Quadrelli, R.: North Atlantic Oscillation response to transient greenhouse gas forcing and the impact on European winter climate: a CMIP2 multi-model assessment, Climate Dynamics, 27, 401–420, https://doi.org/10.1007/s00382-006-0140-x, 2006.

Ulbrich, U. and Christoph, M.: A shift of the NAO and increasing storm track activity over Europe due to anthropogenic greenhouse gas forcing, Climate Dynamics, 15, 551–559, https://doi.org/10.1007/s003820050299, 1999.

Ulbrich, U., Pinto, J. G., Kupfer, H., Leckebusch, G. C., Spangehl, T., and Reyers, M.: Changing Northern Hemisphere Storm Tracks in an Ensemble of IPCC Climate Change Simulations, Journal of Climate, 21, 1669–1679, http://dx.doi.org/10.1175/2007jcli1992.1, 2008.

von Storch, H. and Zwiers, F.: Statistical Analysis in Climate Research, Cambridge University Press, Cambridge, 2003.

von Trentini, F., Leduc, M., and Ludwig, R.: Assessing natural variability in RCM signals: comparison of a multi model EURO-CORDEX ensemble with a 50-member single model large ensemble, Climate Dynamics, https://doi.org/10.1007/s00382-019-04755-8, 2019.

Woollings, T., Hannachi, A., Hoskins, B., and Turner, A.: A Regime View of the North Atlantic Oscillation and Its Response to Anthropogenic Forcing, Journal of Climate, 23, 1291–1307, https://doi.org/10.1175/2009JCLI3087.1, 2010.

Woollings, T., Franzke, C., Hodson, D., Dong, B., Barnes, E., Raible, C., and Pinto, J.: Contrasting interannual and multidecadal NAO variability, Climate Dynamics, 45, https://doi.org/10.1007/s00382-014-2237-y, 2015.

Xu, T., Shi, Z., Wang, H., and An, Z.: Nonstationary impact of the winter North Atlantic Oscillation and the response of mid-latitude Eurasian climate, Theoretical and Applied Climatology, 124, 1–14, https://doi.org/10.1007/s00704-015-1396-z, 2016.

Zwiers, F. and von Storch, H.: On the role of statistics in climate research, International Journal of Climatology, 24, 665–680, https://doi.org/10.1002/joc.1027, 2004.